

# High-resolution X-ray spectroscopy: the coming-of-age

J.S. Kaastra<sup>1,\*</sup>

<sup>1</sup> SRON Netherlands Institute for Space Research, Sorbonnelaan 2, 3584 CA Utrecht, the Netherlands

<sup>2</sup> Leiden Observatory, Leiden University, PO Box 9513, 2300 RA Leiden, the Netherlands

<sup>3</sup> Department of Physics and Astronomy, Universiteit Utrecht, P.O. Box 80000, 3508 TA Utrecht, the Netherlands

Received November 21, 2016, accepted TBD

Published online later

**Key words** Galaxies: active – instrumentation: spectrographs – X-rays: general

Since the launch of Chandra and XMM-Newton, high-resolution X-ray spectra of cosmic sources of all kinds have become available. These spectra have resulted in major scientific breakthroughs. However, due to the techniques used, in general high-quality spectra can only be obtained for the brightest few sources of each class. Moreover, except for the most compact extended sources, like cool core clusters, grating spectra are limited to point sources. Hitomi made another major step forward, in yielding for the first time a high-quality spectrum of an extended source, and improved spectral sensitivity in the Fe-K band. For point sources with the proposed Arcus mission, and for all sources with the launch of Athena, X-ray spectroscopy will become mature. It allows us to extend the investigations from the few handful of brightest sources of each category to a large number of sources far away in space and time, or to get high time-resolution, high-spectral resolution spectra of bright time variable sources.

© 2006 WILEY-VCH Verlag GmbH & Co. KGaA, Weinheim

## 1 Introduction

XMM-Newton has been operational already for more than 16 years. It has made many major achievements with all of its instruments, and as we show in this paper, it is still capable of making great discoveries for the next decade. In this contribution we focus on high-resolution spectroscopy. We briefly mention some spectroscopic highlights of XMM-Newton. We will show the great potential offered by the Hitomi satellite during its short lifetime, and then focus on the prospects for some future X-ray missions. We conclude with prospects for RGS for the next decade.

## 2 X-ray instruments

Present-day X-ray instruments can be subdivided into two classes. The most common instruments have relatively high throughput (effective area) but medium to low spectral resolution. In addition, they can do imaging. Good examples of these instruments are the CCD cameras on XMM-Newton, Chandra, Suzaku and Swift. They constitute the most commonly used type of instrument, because of their sensitivity and imaging capabilities. Best use of them is made in studies of broad-band variability, imaging and surveys of large areas or large number of sources.

For detailed astrophysical modeling, often higher spectral resolution is needed. This is until recently offered exclusively by grating spectrometers, such as the RGS spectrometer on XMM-Newton, and the LETGS and HETGS

spectrometers on board of Chandra. Compared to CCDs, their imaging capabilities are limited (mostly in the cross-dispersion direction of the grating), and their effective area lower. They are most useful for the brightest sources of each class. However, provided sufficient source flux, the amount of astrophysical information that can be obtained from a grating spectrum is very large. Due to the way gratings are designed, they are perfect for point sources but show degraded resolution for spatially extended sources. RGS is currently the best grating spectrometer for extended sources, but it can cope only with sources that are effectively smaller than a few arcminutes, like cool core clusters.

Before considering the prospects for XMM-Newton in the future, we first present a few examples of what has been achieved now with this mission with some of the most prestigious projects.

## 3 XMM-Newton now

XMM-Newton has an impressive track record of scientific discoveries. We have no room to discuss that here in detail. We only mention a few highlights here, and only from the RGS. The most important discovery was the discovery of the lack of large amounts of cooling gas in cool core clusters (Peterson et al. 2001; Tamura et al. 2001; Kaastra et al. 2001). Other important early work was the discovery of soft X-ray line emission from photoionised gas in Seyfert 2 galaxies (Kinkhabwala et al. 2002), and the discovery of unresolved inner shell lines from lowly ionised iron in AGN outflows (Sako et al. 2001), not to mention the important

\* Corresponding author: e-mail: j.s.kaastra@srn.nl

work on stellar coronae (e.g. Brinkman et al. 2001) and other sources. All these papers have  $\sim 150$  citations or more.

XMM-Newton in general and RGS in particular remain capable of making new breakthroughs. The same holds for the grating spectrometers on Chandra. We only mention here the following recent highlights of grating spectroscopy, showing the power of these 17 year old missions: the unambiguous detection of the WHIM in absorption (Nicastrò et al. 2013), outflows from a tidal disruption event (Miller et al. 2015) and the discovery of ultra-fast outflows from Ultra-Luminous X-ray sources (Pinto et al. 2016).

Other prominent work that becomes increasingly more important now the mission ages are the use of large data sets or deep exposures of individual targets, and this is the obvious way to make further progress.

A good example is AGN monitoring, where multiple observations with proper spacing allow to use the physical information contained in the time variability to derive for instance the location of the different spectral components (e.g. Kaastra et al. 2012). The associated stacked spectra yield full insight into the landscape of the AGN environment (Detmers et al. 2011).

Another type of study is the study of the chemical composition of clusters of galaxies; stacking the data of a large number of clusters, and using both RGS and EPIC data, Mernier et al. (2016ab) was able to obtain the most accurate decomposition so far.

Stacked cluster data also can be used for a search of dark matter (Bulbul et al. 2014). This study, focused on the possible detection of an unidentified 3.5 keV line that might be attributed to the decay of sterile neutrinos, a possible form of dark matter, also triggered work on charge exchange emission in clusters (Gu et al. 2015), a more common explanation for the presence of a 3.5 keV line. All this has been possible thanks to the archive of 16 years of XMM-Newton observations.

## 4 Hitomi

With the launch of Hitomi on February 17 from Japan, a new perspective for high-resolution X-ray spectroscopy has opened. The three strongest features of this mission are the following.

First, it is now possible to obtain high-resolution spectra also for spatially extended sources, thanks to the SXS detector, a 6x6 pixel calorimeter array. The first light for this instrument was the Perseus cluster (Hitomi collaboration 2016). For the first time it was possible to directly determine the turbulence in a cluster of galaxies by measuring the line broadening. The measured turbulent velocity in Perseus was  $164 \pm 10$  km/s. Before this, only rather crude upper limits of order 500 km/s were obtained using RGS spectra of clusters (Pinto et al. 2015) or indirect measurements using resonance scattering with RGS could constrain the turbulence somewhat (Werner et al. 2009, De Plaa et al. 2012). However, in the latter case not fully resolved issues

with the precise atomic data made the analysis difficult, and in the former case the relatively low effective spectral resolution for extended sources and instrumental line spread function uncertainties were limiting the conclusions.

The second strength of the SXS instrument of Hitomi was the high spectral resolution in the Fe-K band, not only for clusters of galaxies like Perseus, but also for point sources like active galactic nuclei or X-ray binaries. A barely detected ( $2\sigma$ ) narrow Fe-absorption line in the prototype Seyfert 1 outflow galaxy NGC 3783 using a Ms of Chandra HETGS data would have been surpassed by SXS: in only 20% of that exposure time, it would have rendered a  $20\sigma$  detection. Unfortunately, the Hitomi satellite failed before the first AGN spectrum could be taken.

A third strength, namely simultaneous broad-band sensitivity over the band between 0.3 keV and several 100 keV could also not been proven due to the unfortunate fate of the mission.

Already the Hitomi spectrum of the Perseus cluster has challenged the atomic plasma codes that are being used widely in the X-ray community. Several updates in both the SPEX and APEC codes were needed to get the last bits of information out of this spectrum, and at this spectral resolution, even things like Voigt line profiles, rather than Gaussian approximations, start becoming relevant.

## 5 Future X-ray spectroscopy missions

Due to the unfortunate end of Hitomi, at present only the almost 17 year old grating spectrometers of XMM-Newton and Chandra are our spectroscopic working horses. They are still doing fine, yielding regularly new discoveries (Sect. 3), but we are waiting for other breakthroughs facilitated by new missions.

A Hitomi recovery mission, if approved, could fly early in the next decade around 2020/2021 and would do all the science foreseen for the SXS instrument. Other ideas, for wide field of view, high spectral resolution missions are being considered, like DIOS in Japan or comparable missions in China, but in the former case this may not be independent of the selection of a Hitomi successor. Time will show.

ESA is preparing the Athena mission, a major new flagship to be launched in 2028, with superb capabilities in terms of effective area, imaging qualities and spectral resolution as compared to XMM-Newton. That promising mission is discussed elsewhere (Nandra et al. 2013). Here I want to focus on another mission that might be launched earlier, Arcus. Table 1 compares the relative strengths of several X-ray missions in terms of resolving power and figure of merit for weak line detection.

## 6 The Arcus mission

Arcus is a concept for a NASA Midex proposal; if selected it could fly around 2023. A more detailed description of this

**Table 1** Resolving power ( $R$ ) and figure of merit  $F \equiv \sqrt{RA_{\text{eff}}}$  for weak line detection for existing and future missions compared to Hitomi (which has spectral resolution 5 eV for all energies).

Instrument	$R$	$R$	$R$	$F$	$F$	$F$
E (keV)	0.5	1.5	6	0.5	1.5	6
HRC-S/LETG	6	0.7	0.04	1.3	0.2	0.03
ACIS-S/LETG	6	0.7	0.04	0.5	0.4	0.08
MEG	12	1.4	0.09	0.3	0.6	0.06
HEG	–	3	0.17	–	0.5	0.13
RGS	4	0.5	–	3	0.24	–
SXS Hitomi	$\equiv 1$	$\equiv 1$	$\equiv 1$	$\equiv 1$	$\equiv 1$	$\equiv 1$
Arcus	25	8	–	17	3.5	–
Athena XIFU	2	2	2	19	9	5

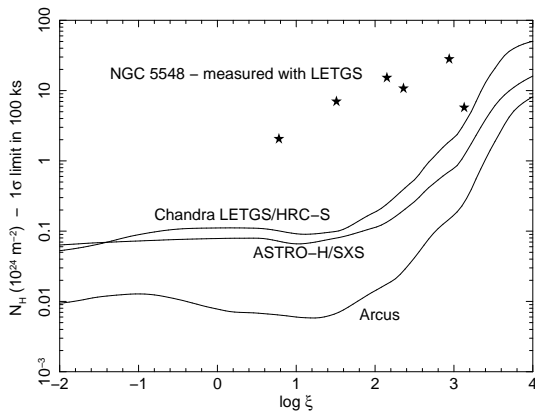


**Fig. 1** Minimum detectable column density of an outflow in 100 ks at the  $1\sigma$  level. See text for details.

mission can be found in Smith et al. (2016). Basically, one may consider it in terms of performance as a mission with ten times the spectral resolution and ten times the effective area of the RGS, operating over a slightly different band between roughly 10–50 Å.

The main science goals are a study of the halo of our Milky way and other galaxies by measuring their absorption spectra towards bright background sources, AGN feedback, and several other interesting science questions. Here I focus on AGN feedback.

Due to the increased sensitivity of Arcus compared to the Chandra or XMM-Newton gratings, much lower column densities can be detected, as illustrated in Fig. 1. We have considered here the column densities of the six photoionised components of the outflow in NGC 5548 in its normal, unobscured state (Kaastra et al. 2014). These are indicated by stars in the figure. We have simulated this spectrum for each of the following instruments for 100 ks exposure time: Chandra LETGS, ASTRO-H (Hitomi) SXS detector, and Arcus. These simulated spectra were fitted over the full band of the instruments with the same model, and the nominal statistical uncertainty of the column density has been determined and is shown in Fig. 1. For ionisation parameters  $\log \xi < 2$  Arcus is about an order of magnitude more sensitive than the other instruments, while for the higher ion-

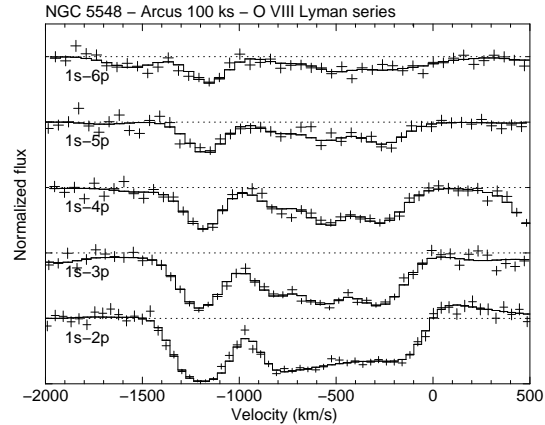


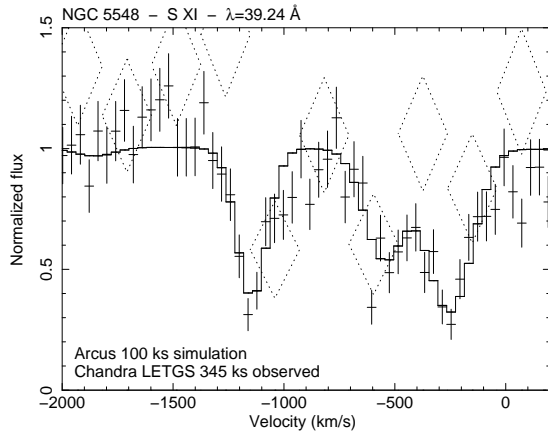
**Fig. 2** Normalized spectra (continuum set to unity) for a 100 ks exposure of NGC 5548 in its normal unobscured state. Individual spectra have been shifted for clarity. The Lyman series of O VIII is shown.

isation parameters it is still more sensitive but to a lesser extend.

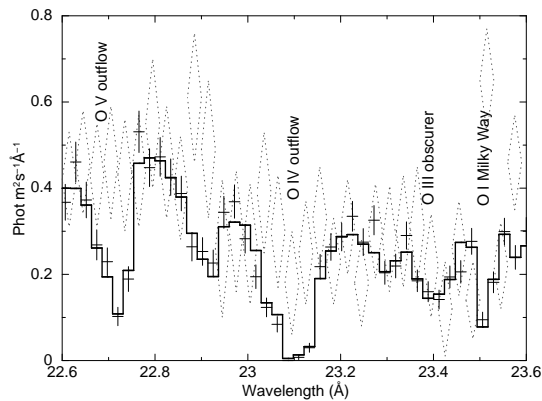
We show the Arcus capabilities for the same source in another way in Fig. 2. It is easy to detect the full Lyman series of ions such as O VIII, and to resolve the lines into all their velocity components. This is a new aspect of Arcus: with the existing grating data (Chandra and XMM-Newton), these lines are not resolved; they only show a small amount of broadening, and from the centroid shifts one may get some impression whether the components at  $-1200 \text{ km s}^{-1}$  are more dominant than those around  $-500 \text{ km s}^{-1}$ . With Arcus we will resolve the spectra down to about  $100 \text{ km s}^{-1}$ , close to their width as can be determined e.g. from UV spectra. However, the great advantage of X-ray spectra compared to UV spectra is the much larger number of ions that are available for diagnostic purposes; in the UV band only a small number of low-ionisation lines can be investigated. Moreover, feedback is stronger at the high ionisation X-ray lines, both due to higher column densities and higher velocities (e.g. Ultra-Fast Outflows).

Fig. 3 shows a part of the Chandra LETGS spectrum of NGC 5548 in its normal state. This instrument is the only instrument so far that is capable of measuring the spectrum beyond 38 Å. It is focused on the strongest S XI line near 39.24 Å. This line was first identified in this spectrum by Steenbrugge et al. (2005), but given the relatively low effective area of the LETGS the detection is not very strong, and rests upon the prediction that it should be there based on stronger lines from other ions at shorter wavelengths. As the figure shows, Arcus will have no problems in detecting the line and even in resolving it into its velocity components that span the range from  $-1200$  to  $0 \text{ km s}^{-1}$ . This line is of interest, because it has nearby lines from the same ion that arise from metastable levels, hence S XI is an excellent density indicator. We elaborate that later in this section.

For decades NGC 5548 has been in a state showing a prototypical outflow that was used for the simula-



**Fig. 3** Observed Chandra LETGS spectrum of NGC 5548 in its normal, unobscured state near the S XI line (exposure time 345 ks, dotted diamonds) and a 100 ks simulation of the same spectrum with Arcus (crosses). The model used for the simulation is indicated by the solid line and is based on the Chandra data (see Kaastra et al. 2014 for details).



**Fig. 4** Part of a simulation of a 660 ks Arcus observation of NGC 5548 in its obscured state (solid line: model; solid crosses: simulated data), compared to the observed 660 ks RGS spectrum (dotted diamonds). The Arcus data have been rebinned by a factor of 10 for this plot in order to match better the RGS resolution. Two absorption lines from the outflow (O V and O IV), a line from the obscurer (O III) and a Galactic foreground line from O I are indicated.

tions shown in Figs. 2–3. However, starting around 2011, the source showed in addition strong obscuration by high-column density, low ionisation material (Kaastra et al. 2014). This obscuring material was close to the broad line region, contrary to the normal outflow that is located at pc-scale distances (Arav et al. 2015, Ebrero et al. 2016).

The obscurer caused a strong lowering of the ionisation parameter of this normal outflow. The direct observational evidence for the obscuring material comes from the UV band, showing broad ( $5000 \text{ km s}^{-1}$ ) outflowing absorption in intermediate ionisation lines, and in X-rays mainly from the continuum opacity of the obscuring material. Because the obscuration is not 100%, a small amount of X-rays still

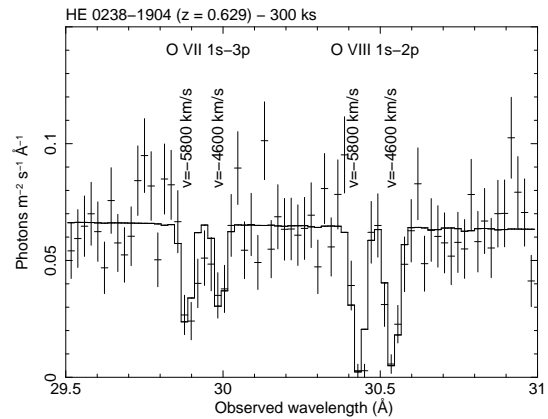


**Fig. 5** Arcus simulation of the spectrum of HE 0238-1904.

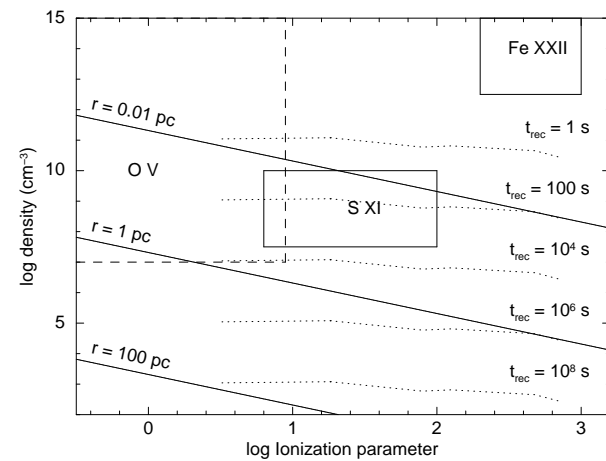


**Fig. 6** Density indicators for AGN outflows. See text for details.

leaks through the soft X-ray band, but the remaining flux is roughly 20 times less than the “normal”, unobscured flux in this band. Due to this effect, RGS was unable to reveal the details of the obscured soft X-ray absorption spectrum; only the emission lines from a region far away from the nucleus remained unobscured and visible. However, the best-fit model predicts that in the soft X-ray band both absorption lines from the normal outflow (at a reduced ionisation parameter) and from the obscurer should be present. This is shown in Fig. 4. The figure shows how well these lines can be seen, and their profiles are resolved by Arcus. This cannot be done with Athena (too low spectral resolution).

The enhanced sensitivity of Arcus not only allows for better (or time-resolved) spectra of the brightest sources, it also allows to study outflows at much larger distances. This is illustrated in Fig. 5, where we show a 300 ks simulation of a redshift 0.629 quasar near the oxygen K-complex. Due to the relatively high redshift, these lines are redshifted from the  $19 \text{ \AA}$  band to the  $30 \text{ \AA}$  band. The simulation is based on the UV spectrum published by Arav et al. (2013). Velocities and ionisation stages can be well separated.

Finally, the enhanced sensitivity of Arcus and its relatively broad wavelength range also will open the doors for a completely new type of diagnostic in AGN outflows: using density sensitive lines. Up to now, density sensitivity has been seen only in some grating spectra of very bright X-ray binaries, e.g. Miller et al. (2008).

In Fig. 6 we give a few examples of density diagnostics for Arcus absorption spectra of AGN, again based on the normal, unobscured spectrum of NGC 5548. In the ionisation parameter versus density plane we plot the regions for which we have density diagnostics. Solid lines indicate lines of equal distance to the ionising source. The dotted lines indicate the densities that can be derived from variability studies: by constraining the recombination time scale through measuring or limiting the lag of the outflow spectrum relative to continuum flux variations. See e.g. Ebrero et al. (2016) for more details. This technique can also be used with current instruments, however it requires a substantial amount of monitoring observations. New are the density diagnostics by O V K-shell lines (Kaastra et al. 2004), indicated by the dashed region, and in particular S XI and Fe XXII. S XI has a few lines in the 39 Å part of the spectrum that are sensitive to relatively low densities; Fe XXII is sensitive to much higher densities.

## 7 What can we do now?

The plans for future missions like a successor for Hitomi, Arcus or Athena are great. Still, at least for the first four years we will have no new spectroscopy mission. Some of the science that we outlined earlier really needs the high-resolution and high throughput, but long, deep spectra of bright sources taken with XMM-Newton can already give new insights. This holds for most classes of objects, as long as systematic calibration limits are not reached. We come back to that in Section 8.

For these deep exposures, all three main instruments of XMM-Newton (RGS, EPIC and the OM) are of importance. A good example of the latter is formed by deep monitoring campaigns of active galactic nuclei. These sources vary on a multitude of time scales: from minutes to decades. In most cases the archive only contains poorly sampled data, or data sampled only at one particular time scale. However, monitoring campaigns cover such time scales and give excellent time-averaged spectra (for Ms-scale exposure times).

The major strength of the XMM-Newton instruments in such campaigns is for EPIC its sensitivity to variability as well as its broad energy range, for RGS the high spectral quality and for OM the additional UV spectrum that is essential to know for photoionisation modelling.

Such campaigns are even more important when they are performed as part of a multi-wavelength campaign including other instruments. For AGN outflow studies, in particular HST with its COS spectrograph, NuSTAR with its high-energy coverage, Swift with its snapshot capability and ground-based facilities are the most important components,

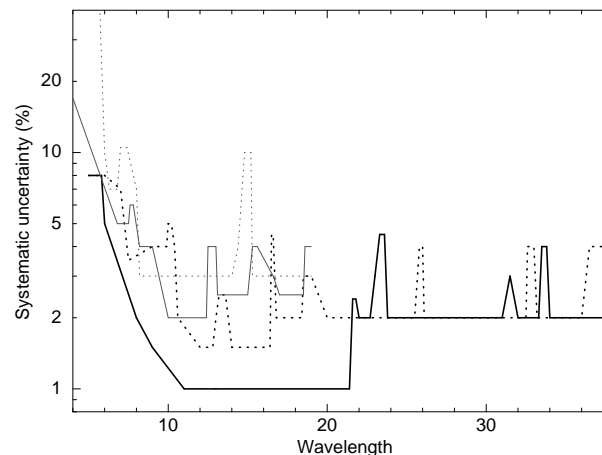


**Fig. 7** Ultimate systematic uncertainties of the RGS effective area as a function of wavelength. Solid lines: RGS1; dashed lines: RGS2; thick lines: first order spectra; thin lines: second order spectra.

apart of course from the XMM-Newton data that form the heart of such campaigns.

With a predicted lifetime of another decade, XMM-Newton has good prospects for performing a number of such projects. However, it is not well known how long the other facilities needed for such work will be operational. Therefore caution must be taken not to delay such projects to near the real end of the mission.

## 8 Limitations imposed by systematic effects

Although still a lot can be learned by making deeper exposures of X-ray sources, there is a natural limitation to how deep one can go. That is given by the exposure time where the statistical uncertainties on the spectrum become smaller than the systematic uncertainties. We have investigated this for RGS as follows.

Within the framework of the RGS calibration, we have derived time- and wavelength dependent correction factors for the RGS effective area. These corrections are based on a detailed study of about a hundred RGS spectra of the blazars Mrk 421 and PKS 2155-304. Space does not allow us to discuss that in detail here. After applying these effective area corrections, there still remains some scatter in the fit residuals for individual spectra. A part of this is of statistical nature and hence of no real concern. However, after correcting for the statistical uncertainties the remaining scatter can be attributed to ultimate systematic uncertainties. We show these uncertainties in Fig. 7.

It is seen that the first order RGS1 spectra have systematic uncertainties of 1–2% over most of the range, while RGS2 has typically 2%. Exceptions are found in some narrower wavelength ranges that are likely due to some remaining slightly unstable pixels or near 32 Å due to time-variable nitrogen contamination. Other exceptions are found at the shortest wavelengths, where it is difficult to model the

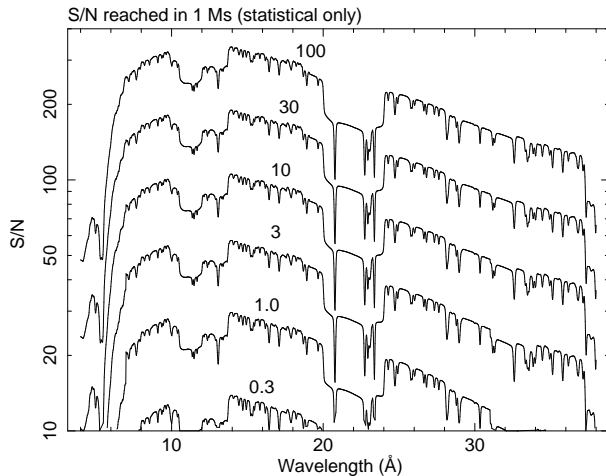


**Fig. 8** Signal to noise ratio per 0.06 Å resolution element for the combined first order RGS detectors that can be achieved in 1 Ms for a continuum source with a flux as labeled. Units of the flux are photons  $\text{m}^{-2} \text{s}^{-1} \text{Å}^{-1}$ .

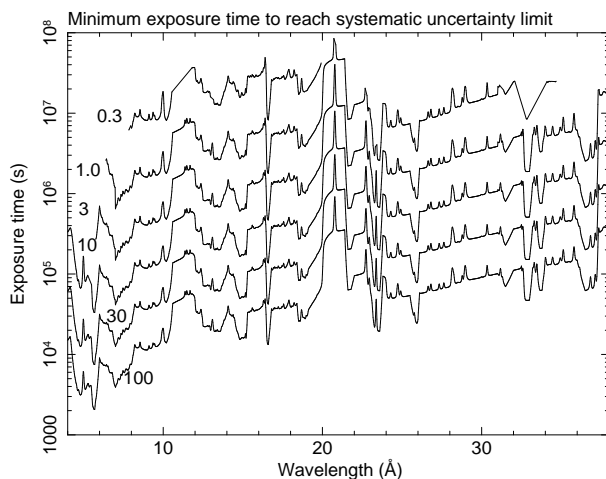


**Fig. 9** Minimum exposure time needed to get a statistical uncertainty per 0.06 Å resolution element equal to the systematic uncertainty in the RGS effective area, for the combined first order RGS detectors, for sources with a flux as labeled. Units of the flux are photons  $\text{m}^{-2} \text{s}^{-1} \text{Å}^{-1}$ .

broad-band grating scattering accurately. For more details about RGS calibration, see also De Vries et al. (2015).

As a next step, we have determined the statistical uncertainties of the flux within a single resolution element of 0.06 Å width, that can be achieved for a source of a given brightness (Fig. 8). In these calculations, a typical quiescent background has been taken into account. That causes the relative low values for the lowest flux considered here of 0.3 photons  $\text{m}^{-2} \text{s}^{-1} \text{Å}^{-1}$ . For even lower fluxes the background becomes dominant. Obviously, it does not make sense to observe the brightest example here (100 photons  $\text{m}^{-2} \text{s}^{-1} \text{Å}^{-1}$ ) for a Ms, because the peak S/N of about 300 corresponds to an uncertainty of 0.3%, much smaller than the systematic uncertainty of the effective area.

For that reason, we have calculated for sources with different fluxes the required exposure time to reach this systematic limit (Fig. 9). For the brightest source this is between 10 and 100 ks; for a typical bright AGN (10 photons  $\text{m}^{-2} \text{s}^{-1} \text{Å}^{-1}$ ) exposure times of a few 100 ks up to about a Ms make sense. Obviously, one can always observe these sources longer if variability rather than spectral quality is the main science driver.

## 9 Conclusions

More than 16 years of XMM-Newton spectroscopy has delivered fascinating science. Even now new topics appear, triggered by carefully investigating the large available databases, serendipitous discoveries and new views made possible by other facilities. While waiting for new missions, XMM-Newton can make significant progress by going deeper and longer in the coming decade.

*Acknowledgements.* SRON is supported financially by NWO, the Netherlands Organization for Scientific Research.

## References

- Arav, N., Borguet, B., Chamberlain, C., Edmonds, D., Danforth, C.: 2013, MNRAS 436, 3286
- Arav, N., Chamberlain, C., Kriss, G.A., et al.: 2015, A&A 577, A37
- Brinkman, A.C., Behar, E., Güdel, M., et al.: 2001, A&A 365, L324
- Bulbul, E., Markevitch, M.L., Foster, A., et al.: 2014, ApJ 789, 13
- Detmers, R.G., Kaastra, J.S., Steenbrugge, K.C., et al.: 2011, A&A 534, A37
- De Plaa, J., Zhuravleva, I., Werner, N., et al.: 2012, A&A 539, A34
- De Vries, C.P., den Herder, J.W., Gabriel, C., et al.: 2015, A&A 573, A128
- Ebrero, J., Kaastra, J.S., Kriss, G.A., et al.: 2016, A&A 587, A129
- Gu, L., Kaastra, J., Raassen, A.J.J., et al.: 2015, A&A 584, L11
- Hitomi collaboration: 2016, Nature 535, 117
- Kaastra, J.S., Ferrigno, C., Tamura, T., et al.: 2001, A&A 365, L99
- Kaastra, J.S., Raassen, A.J.J., Mewe, R., et al.: 2004, A&A 428, 57
- Kaastra, J.S., Detmers, R.G., Mehdipour, M., et al.: 2012, A&A 539, A117
- Kaastra, J.S., Kriss, G.A., Cappi, M., et al.: 2014, Science 345, 64
- Kinkhabwala, A., Sako, M., Behar, E., et al.: 2002, ApJ 575, 732
- Mernier, F., de Plaa, J., Pinto, C., et al.: 2016a, A&A 592, A157
- Mernier, F., de Plaa, J., Pinto, C., et al.: 2016b, A&A, in press (arXiv160803888)
- Miller, J.M., Raymond, J., Reynolds, C.S., et al.: 2008, ApJ 680, 1359
- Miller, J.M., Kaastra, J.S., Miller, C.M., et al.: Nature 526, 542
- Nandra, K., Barret, D., Barcons, X., et al.: 2013, white paper, arXiv1306.2307
- Nicastro, F., Elvis, M., Krongold, Y., et al.: 2013, ApJ 769, 90
- Peterson, J.R., Paerels, F.B.S., Kaastra, J.S., et al.: 2001, A&A 365, L104
- Pinto, C., Sanders, J.S., Werner, N., et al.: 2015, A&A 575, A38
- Pinto, C., Middleton, M., Fabian, A.C.: 2016, Nature, 533, 64
- Sako, M., Kahn, S.M., Behar, E., et al.: 2001, A&A 365, L168
- Smith, R.K., et al.: 2016, proc. SPIE, submitted.

- Steenbrugge, K.C., Kaastra, J.S., Crenshaw, D.M., et al.: 2005, A&A 434, 569
- Tamura, T., Kaastra, J.S., Peterson, J.R., et al., 2001, A&A 365, L87
- Werner, N., Zhuravleva, I., Churazov, E., et al.: 2009, MNRAS 398, 23